# Steep Terrain Ascension Controller for Hexapod Robots

**Thomas Molnar, Ryan Steindl, Navinda Kottege, Fletcher Talbot, Alberto Elfes**
Robotics and Autonomous Systems Group, CSIRO, Pullenvale, QLD 4069, Australia.
{tom.molnar, ryan.steindl, navinda.kottege, fletcher.talbot, alberto.elfes}@csiro.au

## Abstract

Motion of hexapod robots on inclined terrain is an important problem in legged robotics. This paper presents a controller that feeds in to an existing high-level controller with the goal of improving walking performance when ascending inclined terrain. The paper also proposes a new metric, the vertical cost of transport (VCoT), which is a modified form of the conventional energetic cost of transport. This is shown to be an effective measure for comparing inclination ascension performance. The controller implements two behaviours, translating the body in the direction of increasing inclination and adjusting the foot placement during the walking cycle. This is evaluated using a hexapod robot on a range of inclinations, surfaces and gaits. The results show that the controller improves terrain ascension performance with respect to vertical cost of transport, static stability, foot slip and force distribution and identifies the inclination that results in the most efficient ascension of terrain for a given platform.

## 1 Introduction

Legged robots can offer a significant advantage over wheeled or tracked robots when navigating complex terrain [Siciliano and Khatib, 2008]. Their inherent ability to manipulate and interact with terrain in a 3D space makes them a desirable alternative to navigating a variety of complex terrain conditions. In particular, hexapod robots offer a significant advantage in terms of stability and versatility of motion over wheeled robots or even quadruped robots [Roditis *et al.*, 2016]. For a number of real-world tasks, a terrain type that legged robots are expected to navigate is steep terrain.

The bulk of legged robot literature addressing inclined walking has focused on quadruped robots rather than hexapods. Where inclination control is present on hexapods, designs often employ a novel hardware solution [Komsuoglu *et al.*, 2001; Hyungseok *et al.*, 2005; Bartsch *et al.*, 2012] or additional redundant degrees of freedom in their legs [Roennau *et al.*, 2014; Bjelonic *et al.*, 2016]. While these solutions often allow for a much greater versatility in terrain navigation, they come at the cost of increased hardware and software complexity.

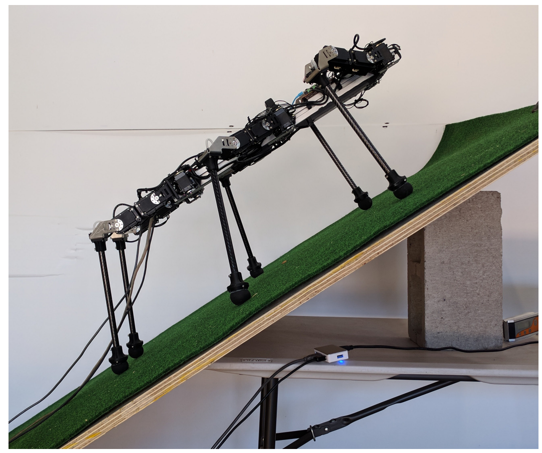

Figure 1: Flexipod, an 18 DoF hexapod, walking on a 30° inclination.

This paper presents the design of a steep terrain controller using a typical hexapod platform to determine the maximum possible performance on steep terrain in terms of stability and energy efficiency.

## 2 Existing Solutions

There exists several prior designs for hexapod robots whose steep terrain performance has been evaluated. Lauron V [Roennau *et al.*, 2014] is a hexapod robot that successfully walked up terrain of 25° and was statically stable on terrain up to 42°. This design implemented many useful control methods including inclination detection and adaptive body posture adjustment. The same concept was extended again in Weaver, a hexapod robot with 5 degrees of freedom (DoF) in each leg [Bjelonic *et al.*, 2016]. Weaver makes use of an online inclination controller, which determines body and ground orientation relative to the gravity vector and adjusts the position of the robot's centre of mass accordingly. Weaver was shown to be able to walk up 30° of incline and maintain static stability up to 50°. In both of these examples, the primary method of adjusting walking for inclinations is reliant on the extra rotational degree of freedom at the Coxa joint in order to rotate the legs to keep them inline with gravity.

Inclined terrain performance in an 18 DoF hexapod was investigated by Wang et al. [2017]. They implement a fuzzy controller that poses the body forward to position the robot's centre of gravity back towards the centre of its projected support polygon. They demonstrate an ability to ascend inclinations that are not possible without the body pose adjustment. Inoue & Kaminogo [2015] proposed two methods to improve terrain navigation. The first was an adjustment of the positions of the middle two legs, which they positioned as far back down the inclination as their operating limits would allow. This was demonstrated to increase stability when climbing, allowing the robot to climb inclinations of up to 35°. The second method they proposed was using shin landing to increase contact area of legs when walking straight up/down inclinations. In this mode the tibia was laid flat when the leg was in contact with the ground. This allowed the robot to navigate up inclinations of 55°. This method is dependent on the ability of the robot to handle ground contact along the length of the tibia. It is also important to note that neither of these papers experimentally measure the efficiency of the slope walking from a cost of transport perspective. Inoue & Kaminogo focuses on quantifying foot slip and Wang et al. uses the static stability margin to test their controller.

Steep terrain ascension has also been investigated in humans. Giovanelli et al used a vertical metabolic cost of walking/running in order to determine the most efficient terrain inclination and gait for inclination ascension in humans. [Giovanelli *et al.*, 2015] They found that for a human optimal terrain ascension is achieved when walking on inclinations between 25°and 30°, with the maximum slope achievable for sustained bipedal motion at approximately 40°.

## 3 Hardware requirements

Due to the wide range of available hardware configurations possible for legged robots, it is important to define the scope of the hardware when designing and evaluating a controller. The following hardware constraints have been imposed:

- The platform utilised in the design will be a typical 18 DoF hexapod robot (Figure 1).
- The only sensory data available to the controller will be the information from the joints (angle, velocity and torque) and an IMU.

The reason for an 18 DoF robot is that 3 DoF per leg is the minimum number to guarantee arbitrary foot-tip positioning in the environment. Constraining the available sensory information to joint states and IMU data ensures the controller is as hardware independent as possible.

## 4 Inclination Controller overview

This investigation into steep terrain ascension makes use of an existing kinematic controller for hexapod robots for the generation of predefined gait walking patterns and leg swing trajectories. The primary focus of this paper is to adjust the walking parameters of the hexapod whilst still allowing the underlying kinematic controller to take care of the motion of the robot. Figure 2 shows how the inclination controller integrates into the existing robot control software environment.

The solution implemented contains two key reactive behaviours that the robot performs when it encounters inclined terrain: *Body translation adjust* and *Foot placement adjust*. The controller uses an IMU, joint states and a feed-forward estimate of ground contact state to determine the angle of the inclined terrain, the robot's pose relative to the plane of inclination and static stability. It then uses this information to adjust its walking parameters.

### 4.1 Body translation adjustment

In this controller the motion of the robot is assumed to be quasi-static. In the static case, the most basic criteria for stability is to keep the robot's centre of gravity between the convex hull of its ground contact points (the support polygon). The minimum distance between the centre of gravity and the boundary of the support

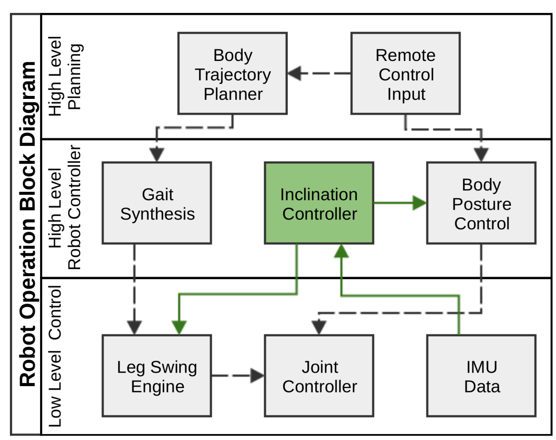


Figure 2: Position of inclination controller in the robot software environment.

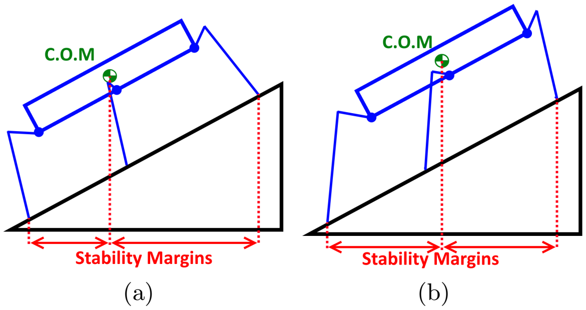


Figure 3: Static stability margins (a) without body translation and (b) with body translation.

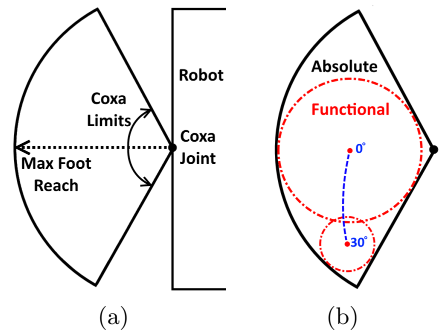


Figure 4: Top down view of (a) absolute workspace calculation and (b) functional workspace calculation for varying inclinations (with interpolation line).

polygon is the static stability margin (SSM) [McGhee and Frank, 1968] [Lee *et al.*, 1988]. A legged robot on uneven or inclined terrain is statically stable if the horizontal projection of its centre of gravity lies within the horizontal projection of its support polygon [Lee *et al.*, 1988] [Zhang and Zhang, 2011]. As inclination increases, the projected support polygon of ground contact points is reduced in dimension along the direction of the slope, with the centre of mass shifted further towards the rear boundary. In order to compensate for this decrease in the static stability margin, the first function that the inclination controller performs is to translate the body in the direction of the inclination to shift its projected centre of mass back towards the centre of the support polygon. This then allows the robot to stand and walk on inclinations that would otherwise cause it to tip over. A diagram of this is shown in figures 3(a) and 3(b). The amount of translation is calculated according to the following formula:

$$x = tan(\theta) \times h \tag{1}$$

Where:

- $x$ = body translation distance (m)
- $h$ = body height when walking (m)
- $\theta$ = inclination angle (rad)

This translation distance value is then passed to the body posture control module of the existing kinematic control software to perform the adjustment during operation.

### 4.2 Foot placement adjust

As the inclination of the terrain increases, the force distribution will become more uneven, with more of the robot's weight being supported by the rear legs. This has two effects; the first being that it disproportionately stresses the joints on the robot, potentially reaching joint torque limits. The second effect is pushing the rear ground contacts closer to their frictional limits, increasing the amount of foot slippage that occurs. The goal of the foot placement adjustment behaviour is to adjust the stance positions of each of the feet during walking in order to mitigate this effect. This adjustment in essence alters the shape of the support polygon during walking.

When discussing foot placement the workspace of each leg must be defined. The workspace considered in this paper is constrained by the circular sector formed on the ground plane by the achievable ground contact points for a given leg. This is shown in figure 4(a). The underlying kinematic controller then models a functional workspace as a circular area inside this region. This is to simplify omnidirectional walking. Placing the feet at the boundaries of the absolute workspace reduces the size of the functional workspace and thus reduces the achievable walking velocity. During level ground walking, the

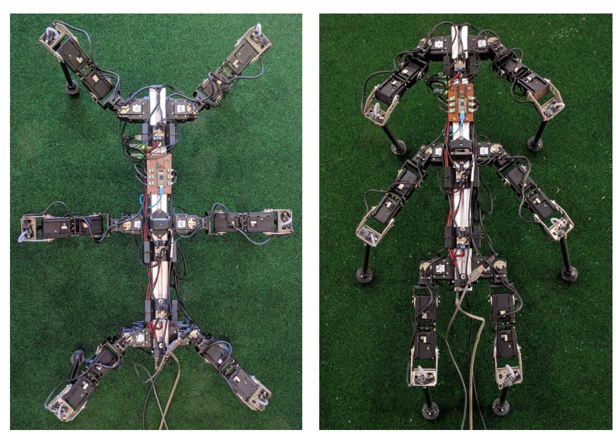

(a) (b)

Figure 5: Position of the feet during (a) flat ground walking and (b) walking on a 30° incline.

default placement of the feet is selected such that it maximises the size of the functional workspace, to allow for the maximum available stride length and thus robot velocity. As the foot moves further away from the centre of its absolute workspace, the stride length available to it decreases and thus so does it's maximum achievable velocity. This introduces a trade off between walking velocity and ascendable inclination when adjusting foot placement. An example of this adjustment is demonstrated in figures 5(a) and 5(b). The determination of an ideal foot placement when walking on inclined terrain is dependent on a number of factors: inclination angle and direction, frictional constraints, as well as the specific morphology of the robot on which the controller is run.

The exact positioning of the feet during operation in this controller was obtained by experimentally determining the feet positioning that allowed the robot to ascend the maximum slope possible. During operation the controller then interpolates between the default foot placement for the robot and this experimentally determined placement based on the detected inclination angle. An example of this is shown in figure 4(b).

Once a new foot placement for a stance leg has been determined by the controller. The next step is to adjust the foot during walking motion. In regular operation, the motion of the feet is handled by the existing kinematic controller, which models a stance a swing trajectory for each foot centered around its default position. The inclination controller ensures that this walking pattern remains uninterrupted by calculating a custom swing trajectory for each foot that moves it from one positioning to another as part of the normal cycle. This ensures that the robot does not need to stop in order to prepare itself to walk on a new inclination since the transition happens as part of the existing walking motion.

# 5 Experiments

## 5.1 Measuring slope walking performance

This paper experimentally evaluates several aspects of slope walking performance. The primary measure for slope performance used in this paper is the energy efficiency of the robot when ascending inclinations. Giovanelli et al. [2015] use a vertical metabolic cost to analyze human inclination ascension. This paper introduces a similar metric that can be applied to robots, called the Vertical Cost of Transport (VCoT). It represents the ratio of total energy consumed by the robot when changing elevation versus the ideal energy expenditure (the change in pure gravitational potential energy). This is defined as:

$$VCoT = \frac{E}{mg\Delta z} = \frac{E}{mgdsin(\theta)} = \frac{CoT}{sin(\theta)} \qquad (2)$$

Where:

- $E$ = total energy consumed
- $m$ = mass of robot
- $g$ = acceleration due to gravity
- $\Delta z$ = total vertical displacement
- $d$ = total displacement in plane of walking
- $\theta$ = inclination angle

The vertical cost of transport is useful in particular for determining the most efficient climbing angle for a particular robot. It also allows climbing performance to be quantified and compared regardless of robot design. For example, a robot with a very high achievable velocity on a shallow incline could have a comparable vertical cost of transport to a robot with a very slow velocity that ascends very steep incline.

Another key measure of walking performance is that of foot slip. As the gradient increases the friction between the feet and the walking surface becomes more critical to maintaining stable motion. Near the limits of this friction the robot feet will begin to slip during the walking cycle, resulting in a decrease in climbing velocity as the robot slips down the slope. In this paper, the slip of the robot is quantified by measuring the total distance travelled (ground truth) vs. the expected feed forward displacement. The ratio between the two then represents the amount of slip that occurred during walking.

Finally, the motor current draw is measured to provide an indication of the amount of strain placed on each motor during walking, so that load distribution can be compared.

## 5.2 Methodology

The experiments were conducted on an 18 DoF hexapod with semi-rigid tibia segments as shown in figure 1. Three different climbing surface were used: plywood, artificial grass and rubber matting. The inclination angles tested were 5°, 10°, 15°, 20°, 25° and 30°. The surfaces were ascended both with and without the inclination controller enabled using 3 different gaits: tripod, amble & wave. Results were averaged over 5 runs for each experiment. For each experiment the following data were recorded:

- Joint states (position, velocity and effort/current)
- IMU data
- Feed-forward body velocity (output from kinematic controller)
- Body pose adjustment and foot tip position
- Static Stability Margin
- Position ground-truth (through laser tracking)
- Total power consumption of the robot

The experimental setup is shown in Figure 6.

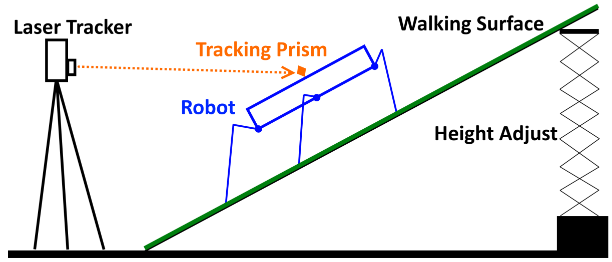


Figure 6: Experimental setup.

### 5.3 Results

Without the controller, the robot was shown to be able to ascend a maximum inclination of 15°, regardless of surface. This was not the result of the robot reaching the boundary of it's static stability, but rather the motors in the rear legs being overloaded from the excessive torque requirements to keep the robot upright. The robot was only able to operate on a 15° slope for a short period of time before the motor's were overloaded. The maximum slope the robot was able to ascend with the controller enabled was 30° for both carpet and rubber, and 25° for plywood. The limiting factor with the controller enabled was friction as the robot feet would slip on higher inclinations, regardless of placement. The results show that the robot reaches a frictional limitation at roughly the same point for all three gaits. The results also showed small variation between surfaces. Thus in the interests of summarising the data appropriately, the results presented below are an average across the 3 surfaces. Additional tabular data showing the results for individual surfaces are included in appendix **??**.

Figure 7 shows the VCoT for each gait, with figure 8 showing additional resolution for tripod and amble gaits. The data shows VCoT is minimised at 15° in all three gaits, both with and without the controller. The controller is shown to improve VCoT for inclinations greater than 10°. At 15° the controller reduces VCoT by 62.3% for wave gait, 34.2% for tripod gait and 3.2% for amble gait. Tripod gait is shown to have the lowest VCoT of all three gaits.

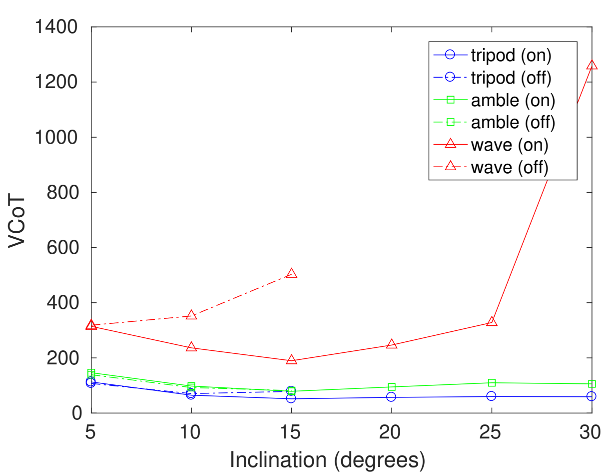


Figure 7: VCoT averaged across 3 surfaces for each gait.

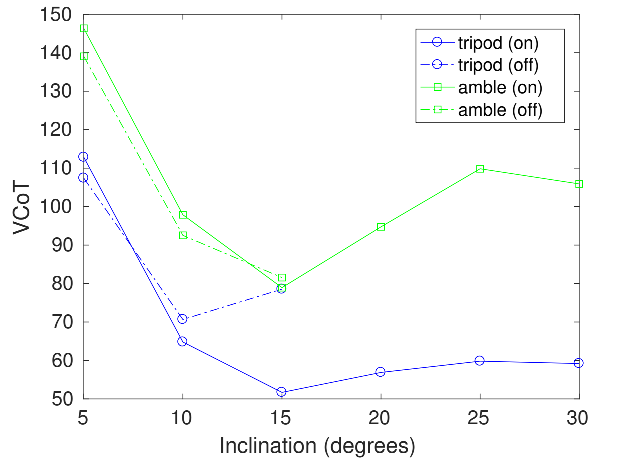


Figure 8: VCoT averaged across 3 surfaces for tripod and amble gait.

Figure 9 shows there is a significant improvement in static stability, with the biggest difference occurring when walking using tripod gait. At 15° this difference becomes pronounced with wave gait showing a 12.1% improvement to SSM, Amble gait a 54.8% percent improvement. The SSM of tripod gait at 15° frequently reached 0 without the controller enabled and the robot would begin to tip backwards down the slope.

Figure 10 shows that foot slip is improved with the controller enabled, with the controller reducing this difference across all three gaits. Tripod gait showed a 19% improvement, Amble an 11.4% improvement and wave gait a 38.4% improvement.

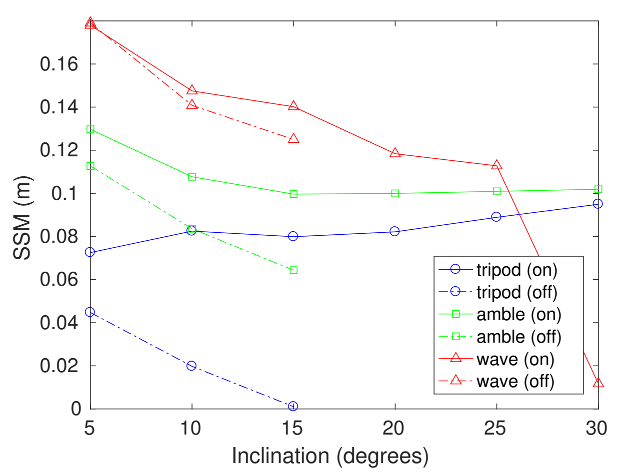


Figure 9: Minimum SSM averaged across 3 surfaces for each gait.

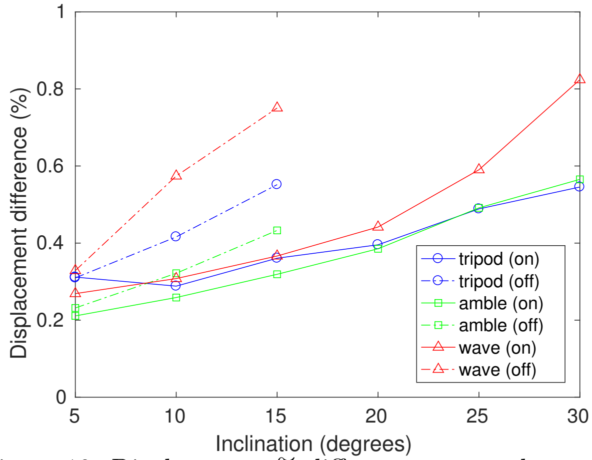


Figure 10: Displacement % difference averaged across 3 surfaces for each gait.

Figures 11, 12 and 13 show the mean and peak current consumed by the motors on the front, middle and rear legs during tripod walking. The data shows reductions in mean and peak current draw for all motors on the front and rear legs on the robot. This is especially true for the rear legs. At 15° in tripod gait, the mean current draw is reduced by 92.4% for coxa motors, 29.8% for femur motors and by 67.4% for tibia motors. Peak current is reduced by 83.4% for coxa motors, 73.0% for femur motors and 62.4% for tibia motors.

## 6 Discussion

The controller is clearly shown to allow the robot to ascend much higher inclinations than would otherwise be possible. This means that the controller can greatly extend the operating envelope of the robot, allowing it to operate in more complicated terrain.

The efficiency of inclination ascension is also clearly

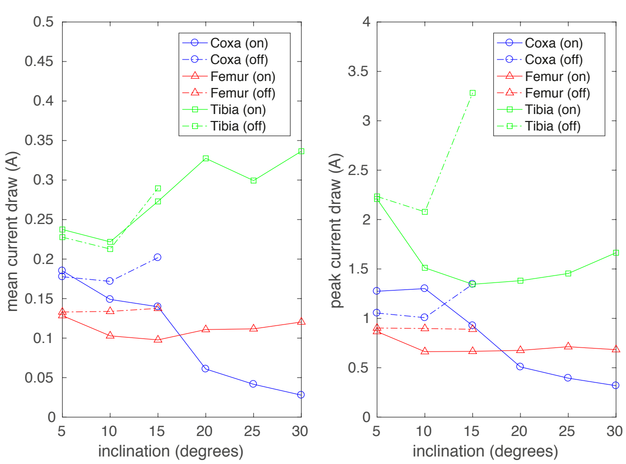


Figure 11: Mean and Peak current on the front legs during in tripod gait

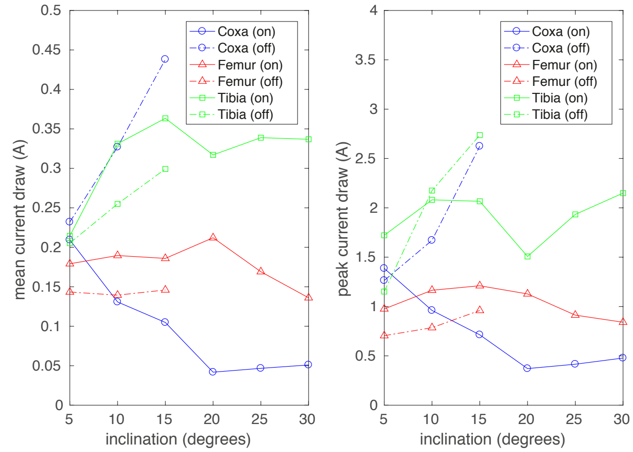


Figure 12: Mean and Peak current on the middle legs during tripod gait

improved, lowering VCoT across all three gaits. Tripod gait is to be expected to have the lower VCoT due to having a faster achievable velocity within a given stride length than either wave or amble gaits. The minimal difference in VCoT in amble gait is an interesting result, as it is in contrast to the other two gaits. The reason for this may be specific to the platform tested, as the robot showed significantly less oscillation of the body when walking in amble gait as opposed to the other two gaits. The semi rigid nature of the legs on the robot combined with the dynamics of amble gait may result in a more stable body motion when walking.

The data shows that the body translation and foot placement improve the static stability margin significantly during walking, with the SSM remaining relatively constant over the 15-30° range in amble and tripod gait with the controller enabled. Without the controller, the robot was shown to operate at the limit of static sta-

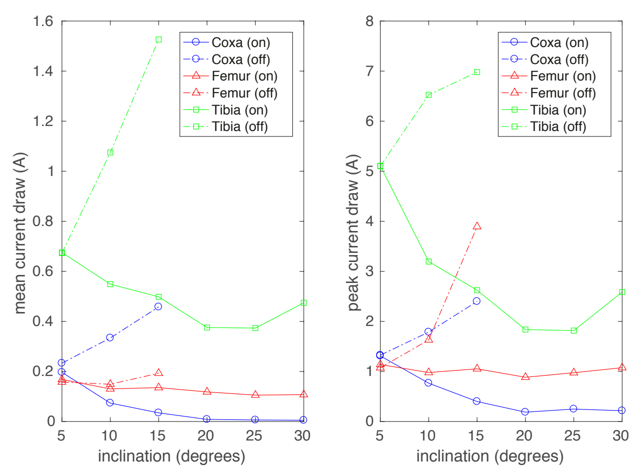


Figure 13: Mean and Peak current on the rear legs during tripod gait

bility with tripod gait at only 15°. The results clearly show that the body translation adjust improves static stability when walking on inclined terrain. The data shows an unexpected drop in SSM at 30° with tripod gait. This may be due to a combination of workspace overshoot and the foot placement at 30°.

The mean and peak current draw data shows that the controller significantly improves loading on the motors during walking on inclines. This supports the approach to improving force distribution through the foot placement adjust. It is also worth noting that the stall current for the motors used in the joints is 6.3 A at 14.8 V, which means that without the controller enabled the stall current was being exceeded by the rear tibia motors during tripod motion at 15°. This indicates that the motors overloading was a primary factor in limited inclination ascension capability without the controller.

These results have significant implications with regard to mission planning, motion planning and navigation, as well as robot design. Knowledge of where VCoT is minimised can allow a high level planner to make decisions about terrain ascension with respect to energy efficiency.

## 7 Conclusions

The controller presented here implemented two simple adjustments which, through only proprioceptive sensing, result in a significant improvement to inclination ascension with respect to energy efficiency, static stability, foot slip and motor load. This paper also proposed the vertical cost of transport as an effective indicator of inclination ascension performance. Further work is currently underway to apply the controller to different hexapod morphologies to verify the utility of the proposed method on multiple robot platforms.

## 8 Acknowledgements

The authors would like to thank David Rytz, Tirthankar Bandyopadhyay and Sebastian Kuppa for their support during the project. This work was fully funded by the CSIRO.

## References

[Bartsch *et al.*, 2012] S. Bartsch, T. Birnschein, M. Römmermann, J. Hilljegerdes, D. Kühn, and F. Kirchner. Development of the sixlegged walking and climbing robot spaceclimber. *Journal of Field Robotics*, 29(3):506–532, 2012.

[Bjelonic *et al.*, 2016] M. Bjelonic, N. Kottege, and P. Beckerle. Proprioceptive control of an overactuated hexapod robot in unstructured terrain. In *2016 IEEE/RSJ International Conference on Intelligent Robots and Systems (IROS)*, pages 2042–2049, 2016.

[Giovanelli *et al.*, 2015] N. Giovanelli, A. L. R. Ortiz, K. Henninger, and R. Kram. Energetics of vertical kilometer foot races; is steeper cheaper? *Journal of Applied Physiology*, 2015.

[Hyungseok *et al.*, 2005] K. Hyungseok, K. Taehun, G. L. Vo, and R. C. Hyouk. Gait planning of quadruped walking and climbing robot for locomotion in 3d environment. In *IEEE International Conference on Robotics and Automation (ICRA)*, pages 2733–2738, 2005.

[Inoue and Kaminogo, 2015] K. Inoue and M. Kaminogo. Steep slope climbing using feet or shins for six-legged robots. In *Asian Control Conference (ASCC)*, pages 1–6, 2015.

[Komsuoglu *et al.*, 2001] H. Komsuoglu, D. McMordie, U. Saranli, N. Moore, M. Buehler, and D. E. Koditschek. Proprioception based behavioral advances in a hexapod robot. In *IEEE International Conference on Robotics and Automation (ICRA)*, pages 3650–3655, 2001.

[Lee *et al.*, 1988] T. T. Lee, C. M. Liao, and T. K. Chen. On the stability properties of hexapod tripod gait. *IEEE Journal on Robotics and Automation*, 4(4):427–434, 1988.

[McGhee and Frank, 1968] R. B. McGhee and A. A. Frank. On the stability properties of quadruped creeping gaits. *Mathematical Biosciences*, 3:331–351, 1968.

[Roditis *et al.*, 2016] I. Roditis, T. Nitsos, A. Porichis, P. Chatzakos, G. Bertos, K. Lika, and E. Papadopoulos. Maintaining static stability and continuous motion in rough terrain hexapod locomotion without terrain mapping. In *Mediterranean Conference on Control and Automation (MED)*, pages 545–550, 2016.

[Roennau *et al.*, 2014] A. Roennau, G. Heppner, M. Nowicki, J. M. Zoellner, and R. Dillmann. Reactive posture behaviors for stable legged locomotion over steep inclines and large obstacles. In *IEEE/RSJ International Conference on Intelligent Robots and Systems*, pages 4888–4894, 2014.

[Siciliano and Khatib, 2008] B. Siciliano and O. Khatib. *Springer handbook of robotics*. Springer, Berlin;London;, 2008.

[Wang *et al.*, 2017] W. Wang, H. Chou, Y. Chen, and R. Lu. Fuzzy control strategy for a hexapod robot walking on an incline. *International Journal of Fuzzy Systems*, Apr 2017.

[Zhang and Zhang, 2011] W. Zhang and L. Zhang. Research of a static balance method for a quadruped robot walking on a slope. In *IEEE International Conference on Information and Automation*, pages 261–266, 2011.